Electronic Supplementary Information

for

A simple method for fabricating drugs containing a *cis*-*o*-diol structure into guanosine-based supramolecular hydrogels for drug delivery

Xin Xia†[a], Shaojuan Song†[a], Yinghui Wen[a], Jiajia Qi[b], Lideng Cao[a], Xian Liu*[a], Ronghui Zhou*[a], Hang Zhao[a]

† These authors contributed equally to this work.

[a] State Key Laboratory of Oral Diseases, National Clinical Research Center for Oral Diseases, Chinese Academy of Medical Sciences Research Unit of Oral Carcinogenesis and Management, Med-X Center for Materials, West China Hospital of Stomatology, Sichuan University, Chengdu, Sichuan, 610041, P. R. China

[b] Oral Biomedical Engineering Laboratory, Shanghai Stomatological Hospital, Fudan University, Shanghai, 200001, P. R. China

* These authors are the corresponding authors.

E-mail: zhouronghui@scu.edu.cn; jssyliuxian@scu.edu.cn

Drug name	Structure of diol			Water solubility	Formation of guanosine-based hydrogel	Stability of hydrogel
	cis-o-diol	*trans-o*-diol	*m*-diol			
Doxifluridine	Y	N	N	G	Y	G
Capecitabine	Y	N	N	G	Y	G
Azacitidine	Y	N	N	G	Y	G
5-Fluorouridine	Y	N	N	G	Y	G
Acadesine	Y	N	N	G	Y	G
Ticagrelor	Y	N	N	G	Y	G
Monocrotaline	Y	N	N	G	Y	G
Mupirocin	Y	N	N	G	Y	G
Luteolin	Y	N	Y	P	N	-
Empagliflozin	N	Y	Y	G	Y	P
Quercitrin	Y	Y	Y	G	Y	P
Naringin	Y	Y	Y	G	Y	P
Baicalin	Y	Y	Y	G	N	-
Entecavir	N	N	Y	G	Y	P
Ganciclovir	N	N	Y	G	Y	P
Pemetrexed	N	N	N	G	N	-

Table 1. Screening of the structural conditions and results of drugs prepared into guanosine-based hydrogels. Y=Yes, N=No, G=Good, P=Poor.

pH	Zero-order		First-order		Higuchi		Ritger-Peppas	
	K_0	R^2	K_1	R^2	K_H	R^2	K_R	R^2
5.4	0.0752	0.9532	-0.225	0.9842	0.2744	0.9798	0.5188	0.9022
6.4	0.0739	0.8535	-0.2408	0.9749	0.2843	0.9731	0.5373	0.9408
7.4	0.0711	0.9557	-0.185	0.9883	0.2599	0.9863	0.5165	0.9339
8.4	0.0649	0.9528	-0.1427	0.9971	0.2383	0.9894	0.5142	0.9534

Table 2. Kinetic parameters of four models (Zero-order, First-order, Higuchi, and Ritger-Peppas) in fitting the release data of Dfu from the GBDfu Hydrogel. (***K*** represents the rate of release, R^2 evaluated the fitness of model in fitting data.)

pH	Zero-order		First-order		Higuchi		Ritger-Peppas	
	K_0	R^2	K_1	R^2	K_H	R^2	K_R	R^2
5.4	0.0135	0.7262	-0.061	0.9724	0.126	0.9154	0.3949	0.9334
6.4	0.0139	0.7966	-0.0478	0.9831	0.1257	0.9642	0.4533	0.9567
7.4	0.0117	0.8341	-0.026	0.956	0.1048	0.9739	0.4399	0.9799
8.4	0.0003	0.8053	-0.0003	0.8068	0.0023	0.9555	0.4984	0.9475

Table 3. Kinetic parameters of four models (Zero-order, First-order, Higuchi, and Ritger-Peppas) in fitting the release data of Dfu from the GPBDfu Hydrogel. (***K*** represents the rate of release, R^2 evaluated the fitness of model in fitting data.)

Loading mode	Drug	Drug release	Synthetic step	Efficiency	Drug activity	References
Physical encapsulation	Doxorubicin	Rapid	3	Low	-	10
Physical encapsulation	5-Fluorouracil	Rapid	4	Low	Active	11
Covalent cross-linking	5-Fluorouracil	Slow	4	Low	Decrease	12
Covalent cross-linking	Taxol	Slow	5	Low	Decrease	13
Borate ester bond	Isoguanosine	Medium	1	High	Active	24
Borate ester bond	Drugs with a *cis-o*-diol	Medium	1	High	Active	This method

Table 4. Comparison with other methodologies.

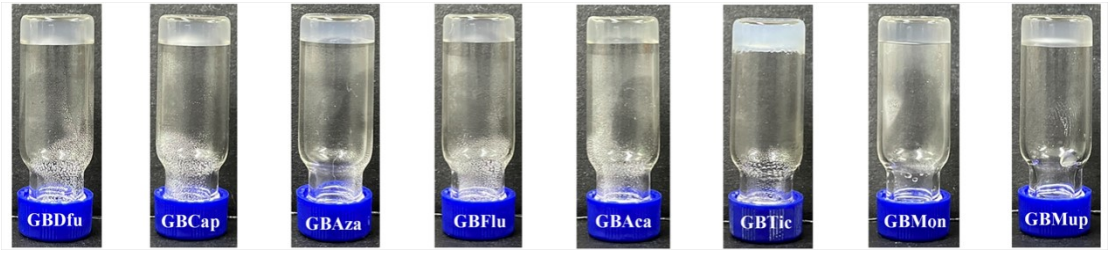

Figure S1. The stability of hydrogels over 6 months.

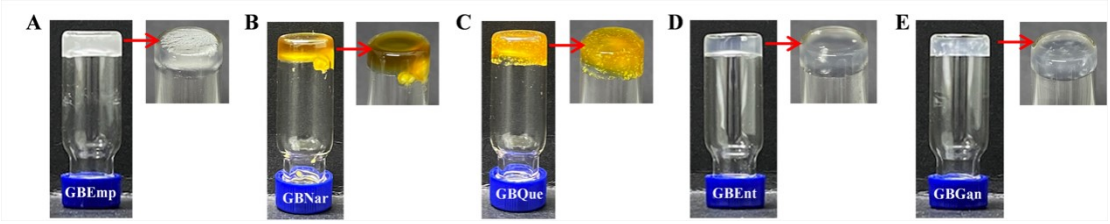

Figure S2. These hydrogels precipitated in different degrees within the first day after preparation. (A) GBEmp, (B) GBNar, (C) GBQue, (D) GBEnt, (E) GBGan.

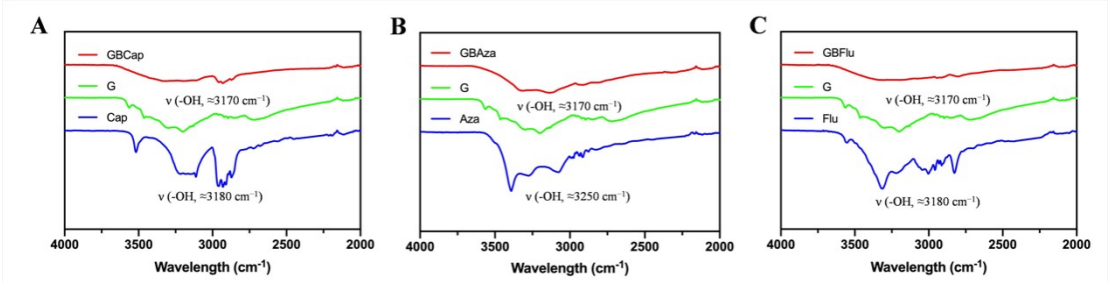

Figure S3. (A) FTIR spectra of G, Cap and GBCap. (B) FTIR spectra of G, Aza and GBAza. (C) FTIR spectra of G, Flu and GBFlu.

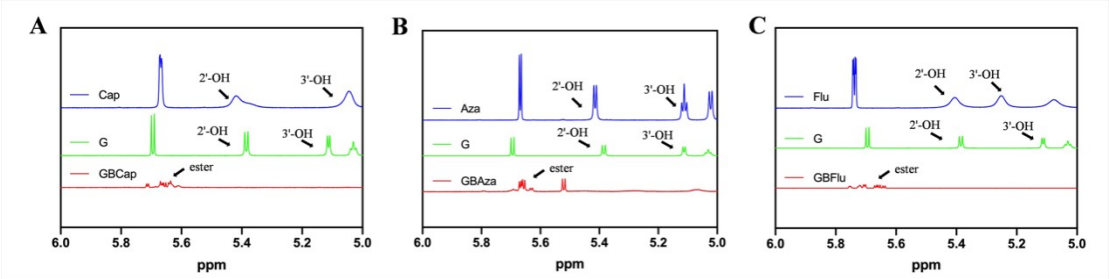

Figure S4. (A) ^{1}H NMR spectra of G, Cap and GBCap in DMSO. (B) ^{1}H NMR spectra of G, Aza and GBAza in DMSO. (C) ^{1}H NMR spectra of G, Flu and GBFlu in DMSO.

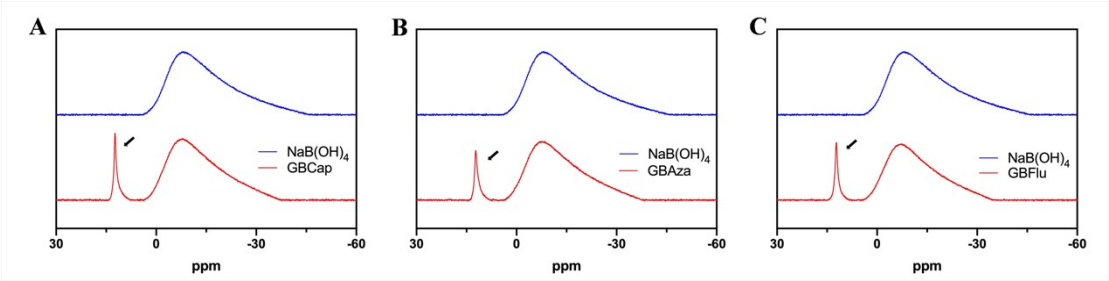

Figure S5. (A) ^{11}B NMR spectra of G, Cap and GBCap in DMSO. (B) ^{11}B NMR spectra of G, Aza and GBAza in DMSO. (C) ^{11}B NMR spectra of G, Flu and GBFlu in DMSO.

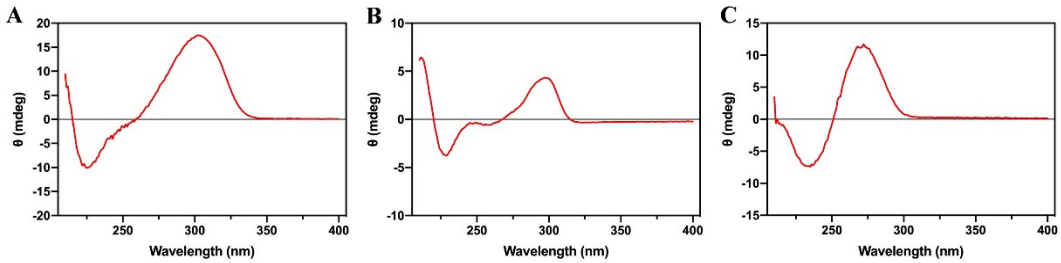

Figure S6. The CD spectra of hydrogels. (A) GBCap, (B) GBAza, (C) GBFlu.

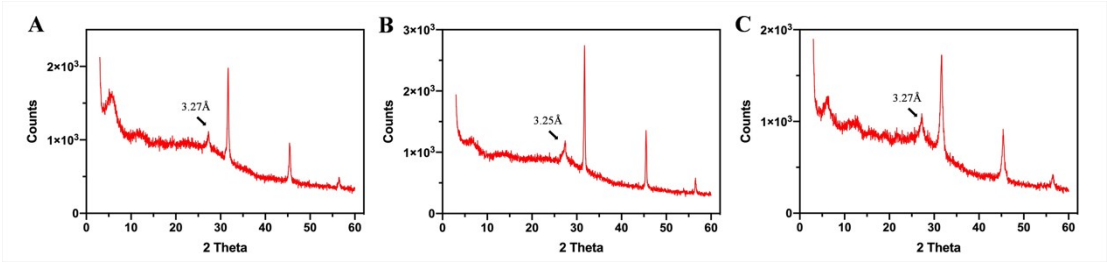

Figure S7. The PXRD spectrum of hydrogels. (A) GBCap, (B) GBAza, (C) GBFlu.

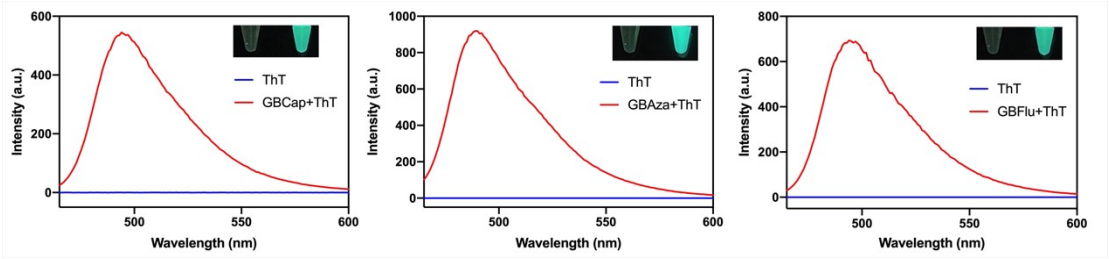

Figure S8. (A) Fluorescence emission spectra of ThT in PBS and GBCap hydrogel. (B) Fluorescence emission spectra of ThT in PBS and GBAza hydrogel. (C) Fluorescence emission spectra of ThT in PBS and GBFlu hydrogel.

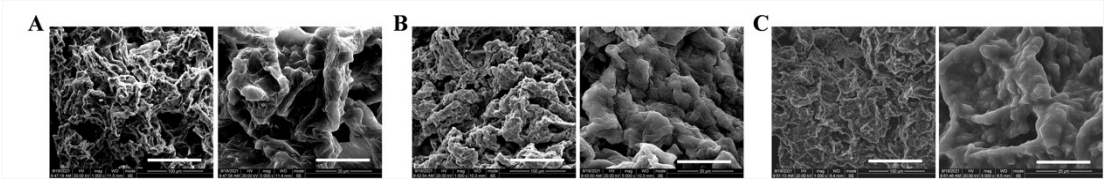

Figure S9. SEM images of the freeze-dried sample of hydrogels. (A) GBCap, (B) GBAza, (C) GBFlu. Scale bar: 100 μm and 20 μm.

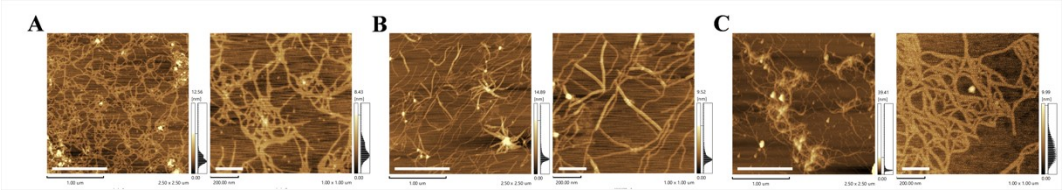

Figure S10. AFM images of the diluted liquid of hydrogels. (A) GBCap, (B) GBAza, (C) GBFlu. Scale bar: 1 μm and 200 nm.

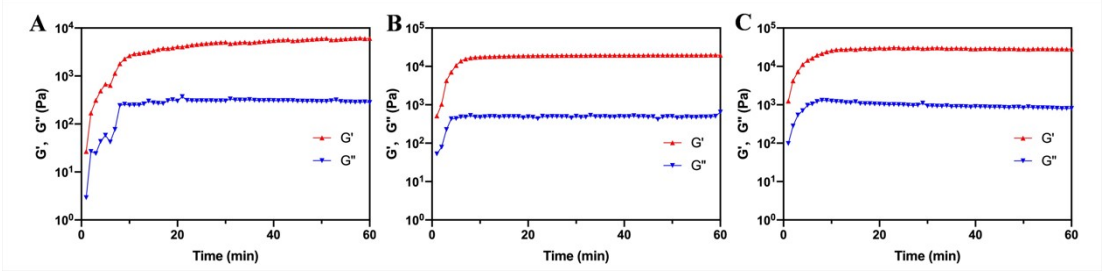

Figure S11. Time sweep of hydrogels. (A) GBCap, (B) GBAza, (C) GBFlu.

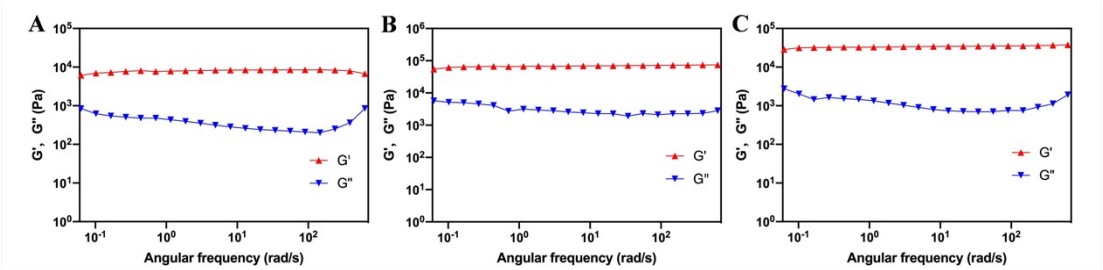

Figure S12. Frequency sweep of hydrogels. (A) GBCap, (B) GBAza, (C) GBFlu.

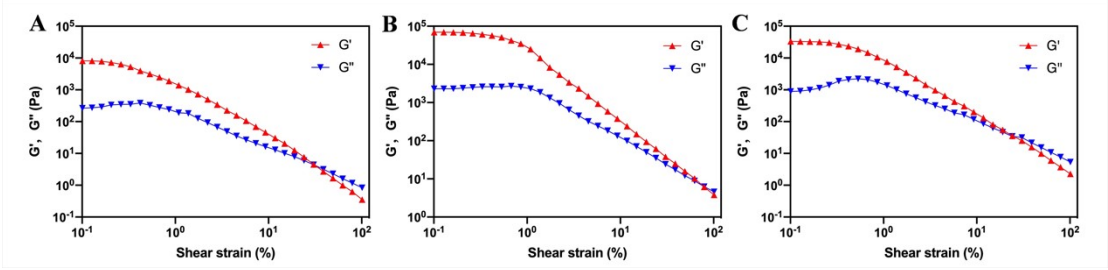

Figure S13. Strain sweep of hydrogels. (A) GBCap, (B) GBAza, (C) GBFlu.

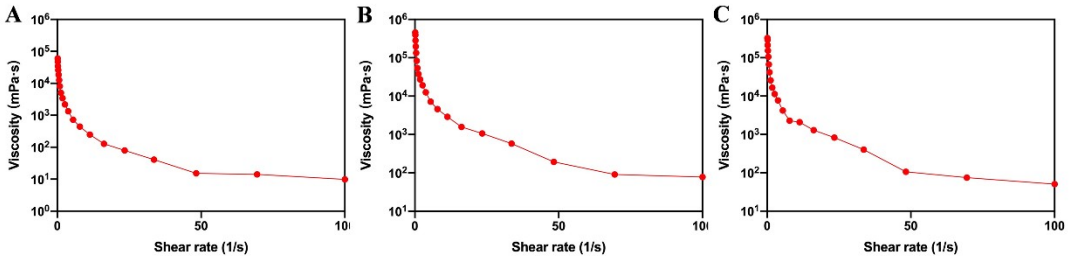

Figure S14. Self-healing test of hydrogels. (A) GBCap, (B) GBAza, (C) GBFlu.

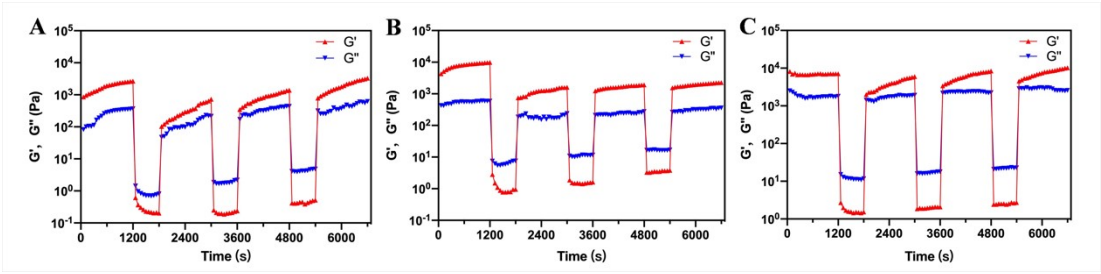

Figure S15. Viscosity test of hydrogels. (A) GBCap, (B) GBAza, (C) GBFlu.

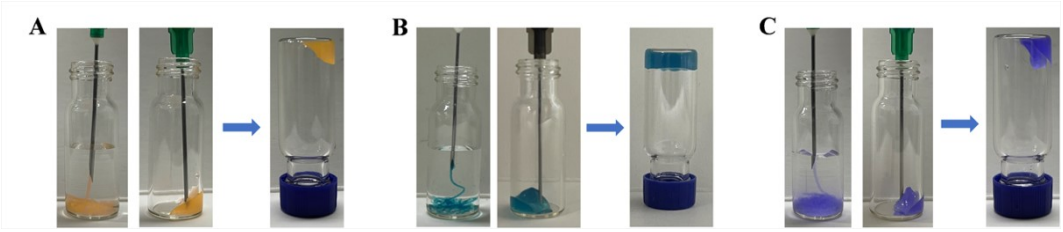

Figure S16. Injectable behavior of hydrogels injected with a 10 mL syringe. (A) GBCap, (B) GBAza, (C) GBFlu.

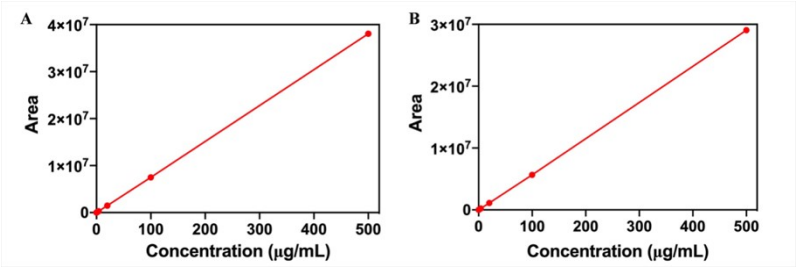

Figure S17. Standard curve of drugs measured by HPLC. (A) Standard curve of doxifluridine: f(x)=76141.0*x-34257.9 (R^2=0.9999903). (B) Standard curve of capecitabine: f(x)=58147.5*x-39075.0 (R^2=0.9999775).

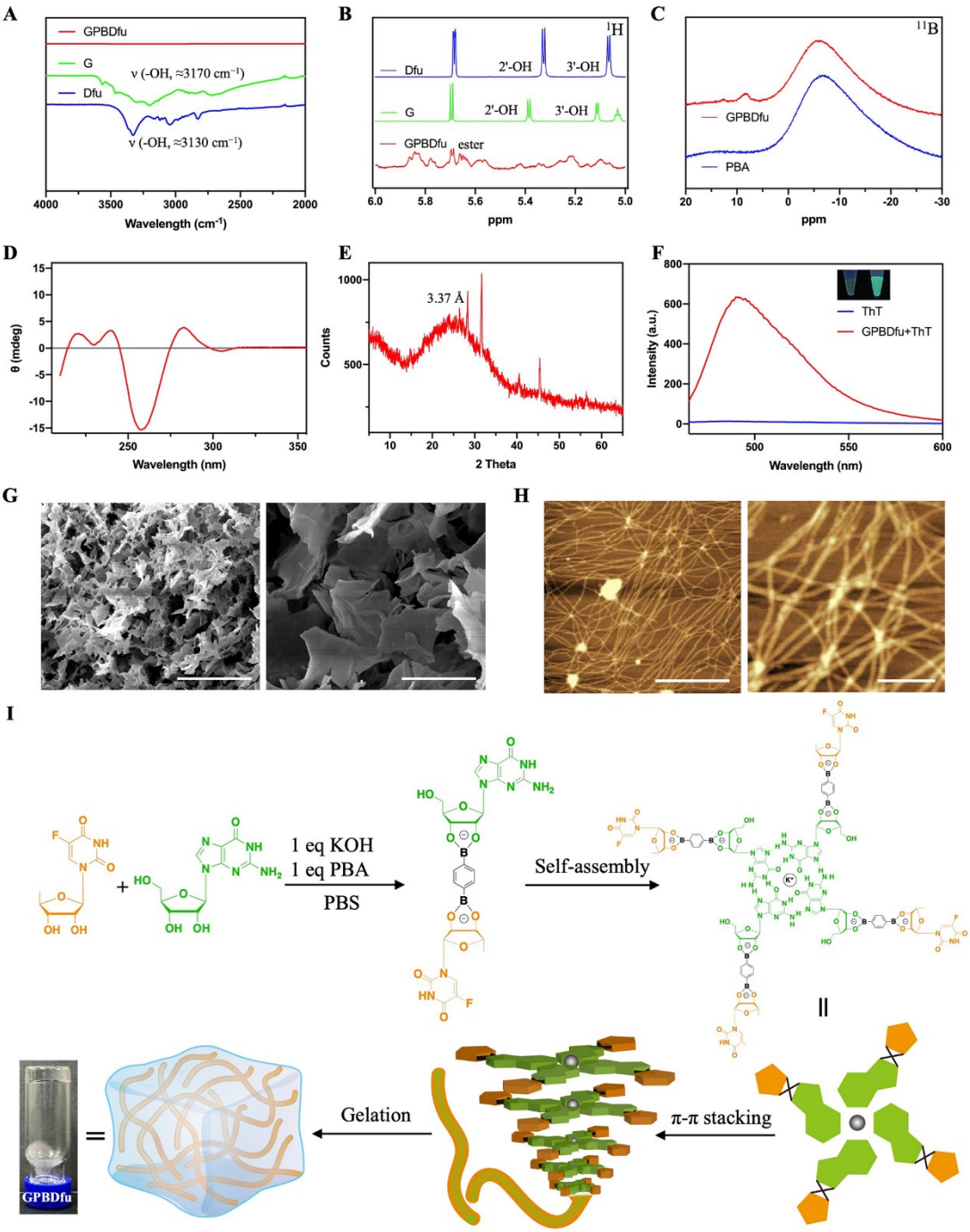

Figure S18. Confirmation of the chemical and microscopic structure of the GPBDfu hydrogel. (A) FTIR spectra of G, Dfu and GPBDfu. (B) ^{1}H NMR spectra of G, Dfu and GPBDfu in DMSO. (C) ^{11}B NMR spectra of PBA and GPBDfu in DMSO. (D) CD spectra of GPBDfu hydrogel. (E) PXRD spectrum of a lyophilized GPBDfu hydrogel. (F) Fluorescence emission spectra of ThT in PBS and GPBDfu hydrogel. (G) SEM images of the freeze-dried sample of GPBDfu hydrogel. Scale bar: 100 μm and 20 μm. (H) AFM images of the diluted liquid of GPBDfu hydrogel. Scale bar: 1 μm and 200 nm. (I) Schematic illustration of the synthesis of GPBDfu hydrogel.

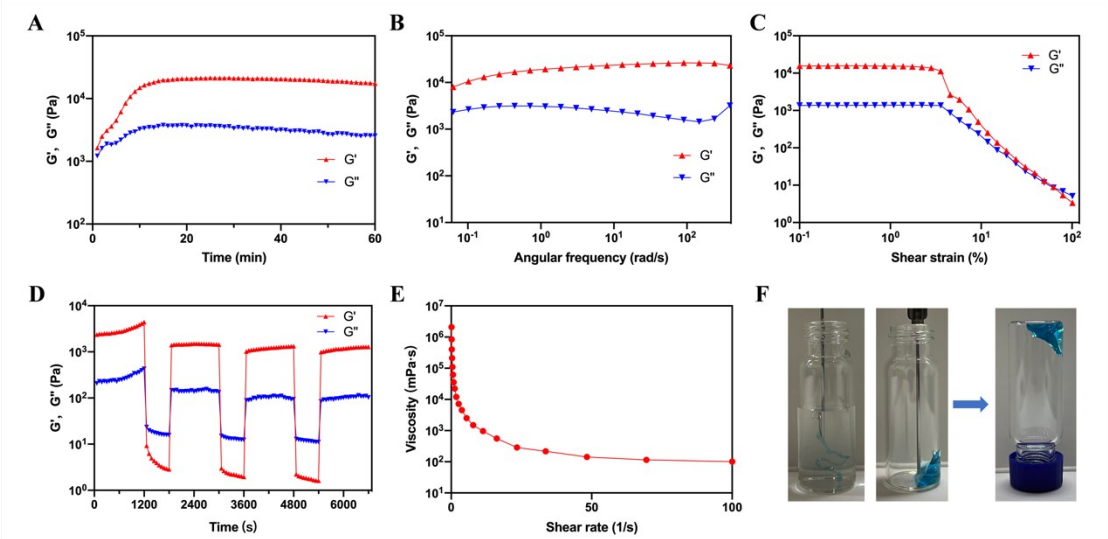

Figure S19. Rheological and injectable experiments of the GPBDfu hydrogel. (A) Time sweep of GPBDfu hydrogel. (B) Frequency sweep of GPBDfu hydrogel. (C) Strain sweep of GPBDfu hydrogel. (D) Self-healing test of GPBDfu hydrogel. (E) Viscosity test of GPBDfu hydrogel. (F) Injectable behavior of GPBDfu hydrogel injected with a syringe.

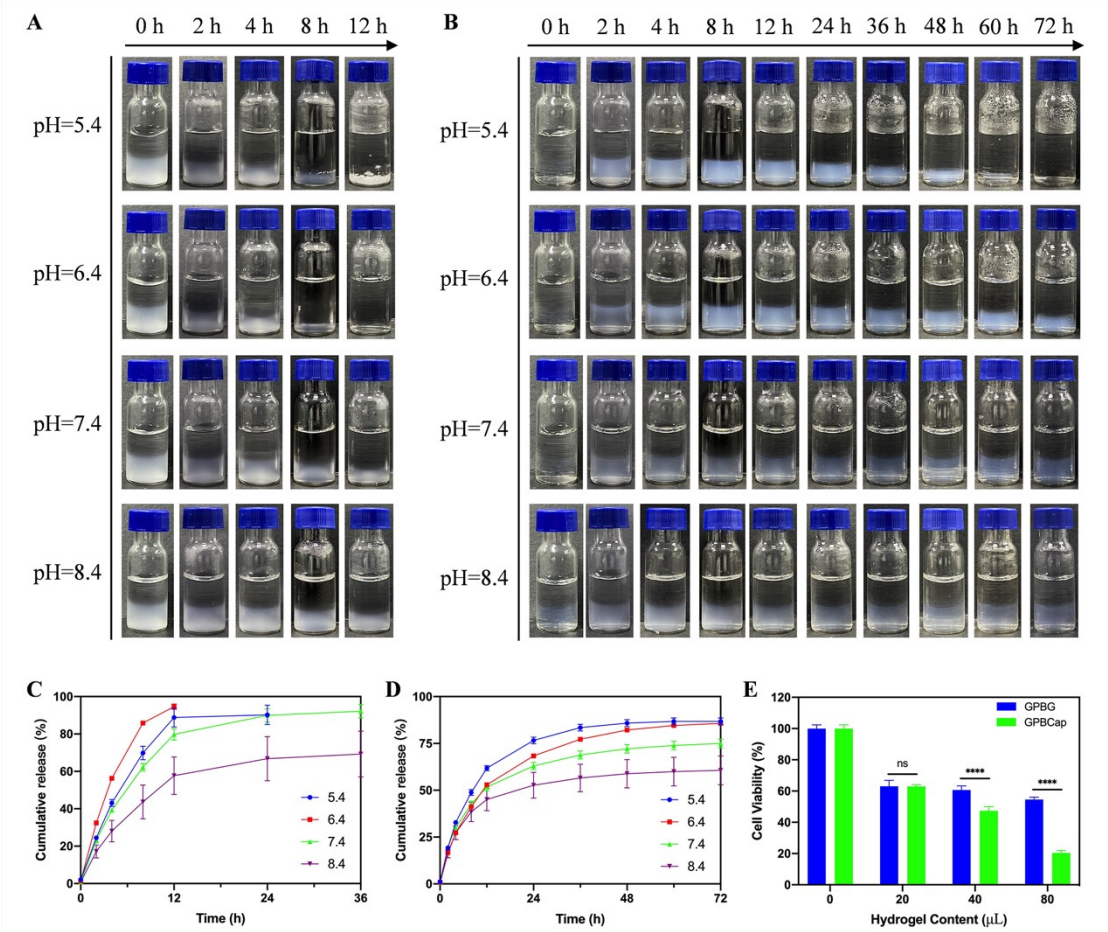

Figure S20. Comparison of sustained drug release performance between GBCap and GPBCap hydrogels. (A) Diagrams of the drug release of GBCap hydrogels in PBS with different pH. (B) Diagrams of the drug release of GPBCap hydrogels in PBS with different pH. (C) Drug release curve of GBCap at different pH conditions. (D) Drug release curve of GPBCap at different pH conditions. (E) Cell viability of the Cal-27 cells treated with GPBG and GPBCap hydrogels at different content for 24 h were measured by CCK-8 assay. Data are given as mean ± SEM (*$p < 0.05$, **$p < 0.01$, ***$p < 0.001$, ****$p < 0.0001$) from three replicates.

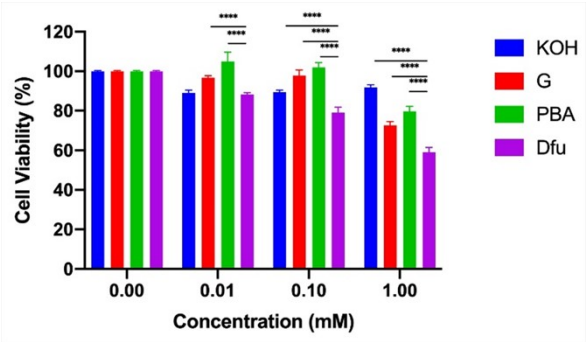

Figure S21. Inhibitory effects of KOH, G, PBA, and Dfu on the growth of Cal-27. Data are given as mean ± SEM (*p < 0.05, **p < 0.01, ***p < 0.001, ****p < 0.0001) from three replicates.